Artificial Intelligence in Geosciences 4 (2023) 22–27

Contents lists available at ScienceDirect

Artificial Intelligence in Geosciences

journal homepage: www.keaipublishing.com/en/journals/artificial-intelligence-in-geosciences

Unsupervised pre-stack seismic facies analysis constrained by spatial continuity

Yifeng Fei *, Hanpeng Cai, Junhui Yang, Jiandong Liang, Guangmin Hu

School of Resources and Environment, University of Electronic Science and Technology of China, China

A B S T R A C T

Seismic facies analysis plays important roles in geological research, especially in sedimentary environment identification. Traditional method is mainly based on seismic waveform or attributes of a single seismic gather to classify the seismic facies. Ignoring the correlation between adjacent seismic gathers leads to poor lateral continuities in generated facies map, which cannot fit the sedimentary characteristics well. In fact, according to sedimentology theory, the horizontal continuities of the stratum can be utilized as priori information to provide more information for waveform classification. Therefore, we develop an unsupervised method for pre-stack seismic facies analysis, which is constrained by spatial continuity. The proposed method establishes a probabilistic model to characterize the correlation between neighboring reflection elements. Subsequently, this correlation is used as a regularization term to modify the objective function of the clustering algorithm, allowing the mode assignment of reflective elements to be influenced by the labels of their neighbors. Test on synthetic data confirms that, compared with traditional seismic facies analysis methods, the facies maps generated by the proposed method have more continuous and homogeneous textures, and less uncertainty on the boundary. The test on actual seismic data further confirms that the proposed method can describe more details of the distribution of lithological bodies of interest. The proposed method is an effective tool for pre-stack seismic facies analysis.

1. Introduction

Seismic facies analysis provides an effective way of determining lithofacies and sedimentary environments. It mainly divides the seismic sequence, and then extracts and analyzes the characteristics of seismic signals in the divided sequence. After that, seismic facies units with similar characteristics are classified into the same category, representing a type of sedimentary properties and sedimentary environment (Alsadi, 2016). Waveform classification and multi-attribute classification are common methods for seismic facies analysis at present (Xu and Haq, 2022), but these methods mostly use the seismic signal of a single reflector as data input, ignoring the correlation of seismic signals of adjacent reflectors. According to the relevant theory of sedimentology, adjacent reflectors have a high correlation in the characteristics of the reflection mode. The lack of consideration of this may make existing analysis methods susceptible to noise interference and leading to poor results (Li et al., 2022).

Restricted by the band-limited seismic acquisition and the characteristics of seismic data itself, it is difficult to obtain sufficient high-quality labeled data sets for supervised learning, so unsupervised algorithms have received extensive attention in the field of seismic data interpretation (Qian et al., 2018; Mousavi et al., 2019; Gao et al., 2021). As an effective clustering algorithm, the fuzzy c-means clustering (FCM) algorithm is widely used. It obtains the membership degree of each data point or data sample to all class centers by optimizing an objective function, so as to determine the categories of the samples to achieve the purpose of automatically classifying the sample data. In recent years, it has been successfully applied to the field of seismic facies analysis and achieved acceptable results (Liu et al., 2022; Mirzakhanian and Hashemi, 2022). However, FCM is sensitive to noise, which has a negative impact on the application of the algorithm in seismic facies analysis. Due to the influence of seismic data acquisition methods and other aspects, even preprocessed seismic data often contain a lot of noise. This often makes the boundaries of FCM results on seismic data unclear and the continuity of clustering is poor, which does not conform to the actual stratigraphic deposition and geological laws.

* Corresponding author.
E-mail address: yifengfei1995@gmail.com (Y. Fei).

https://doi.org/10.1016/j.aiig.2023.01.003
Received 20 December 2022; Received in revised form 16 January 2023; Accepted 19 January 2023
Available online 10 February 2023

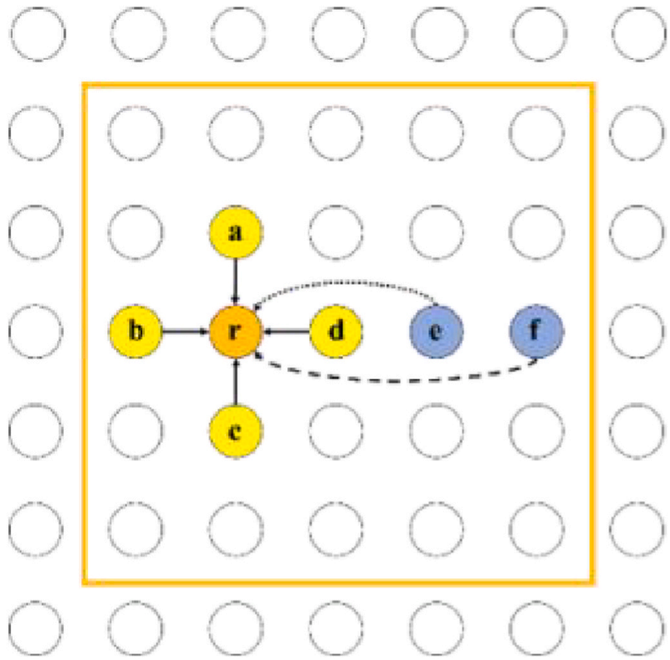

Fig. 1. Illustration of the correlation relationship between different reflectors in the formation. In the selected window (inside the orange box), a, b, c, d are directly related to r, while e and f are indirectly related to r.

According to the theory of geology and stratigraphic sedimentology, there is a strong correlation between the seismic signals of adjacent reflection elements. This can be used as prior information to provide more knowledge constraints for seismic facies classification, improve the lateral continuity of the seismic facies map and enhance the robustness of the algorithm. During the sedimentary evolution of the formation, it is often accompanied by the formation of anomalous bodies, resulting in the formation of karst caves, faults and other structures in the formation. Therefore, the correlation between adjacent reflection elements cannot be represented by hard division (Su-Mei et al., 2022). So we established a probabilistic model to characterize this correlation, and then we used cross-entropy as a distance measurement, fused it into the loss function of FCM, and proposed a novel seismic facies analytical method.

2. Method

Using the standard FCM algorithm to cluster N samples into K clusters, the following objective function is used:

$$\mathrm{J} = \sum_{i=1}^{N}\sum_{k=1}^{K} u_{ik}^{q}\|x_i - v_k\|^2 \quad \sum_{k=1}^{K} u_{ik} = 1\forall i \tag{1}$$

where x_i represents the i^{th} sample, v_k represents the k^{th} cluster center. v_k and x_i have the same feature dimension. u_{ik} represents the probability that the i^{th} sample x_i belongs to the k^{th} cluster center v_k. q is a weighted index, which is generally specified manually.

Fuzzy c-means clustering is calculated using an iterative convergence method, and the values of iterative u_{ik} and v_k are continuously updated through the following equations. When the maximum change value of u_{ik} and v_k calculated twice before and after does not exceed a given threshold, the objective function is converged, and it can be considered that the clustering result has reached the optimum.

$$\mathrm{u}_{ik} = \frac{\sum_{j=1}^{K}\left(x_i - v_j\right)^{\frac{2}{q-1}}}{\left(x_i - v_k\right)^{\frac{2}{q-1}}} \tag{2}$$

$$v_k = \frac{\sum_{i=1}^{N}\left(u_{ik}\right)^q x_i}{\sum_{i=1}^{N}\left(u_{ik}\right)^q} \tag{3}$$

According to the theory of stratigraphic sedimentology, the strata have certain lateral continuity. Therefore, in this paper, we try to establish a probabilistic model to characterize the correlation between such adjacent reflection meta-seismic signals. Briefly, the model should have the following characteristics. 1) The seismic signals of adjacent reflectors are likely to have the same type. 2) The correlation of seismic signals of different reflection elements will weaken with the increase in distance. 3) The correlation between the seismic signals of two reflectors far away should be negligible. To prevent the division error of seismic facies caused by hard division, we choose to use the method of recursive probability estimation to characterize this correlation (Liu et al., 2022). In order to simplify the analysis of this problem, we use the first-order neighborhood system to analyze the different reflectors, as shown in Fig. 1. Here, we assume that the correlation of adjacent reflectors in the first-order neighborhood is direct, while the correlation of non-neighboring reflectors is indirect, and the correlation is limited to the window of our selected area. As shown in Fig. 1, in the selected window, **a**, **b**, **c,** and **d** in the first-order neighborhood of **r** are directly related to **r**, while **e** and **f** are indirectly.

Assume that a certain seismic facies map contains K seismic facies. We define a parameter α related to the probability to characterize the correlation between seismic signals of different reflectors x_h and x_r in the first-order neighborhood.

$$\mathrm{P}(x_h = k | x_r = k) = \alpha \quad \mathrm{k} \in \{1, 2, ..., K\} \tag{4}$$

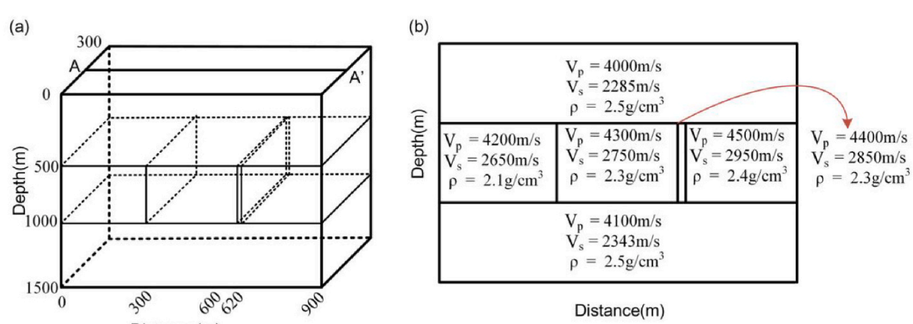

Fig. 2. (a) 3D view of the physical model. (b)The physical model parameters of the section along the AA' line, including S-wave propagation velocity, P-wave propagation velocity, and medium density.

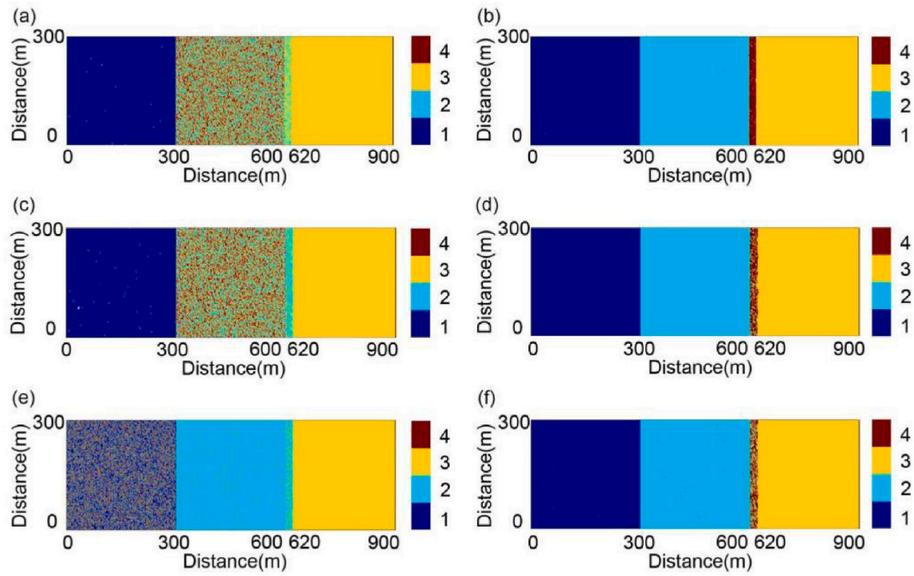

Fig. 3. Seismic facies maps with different Gaussian noise. (a), (c), and (e) show the seismic facies maps obtained by FCM method for 6 dB, 4 dB and 2 dB synthetic data. (b), (d), and (f) show the seismic facies maps generated by FCM-CEC method for the corresponding data.

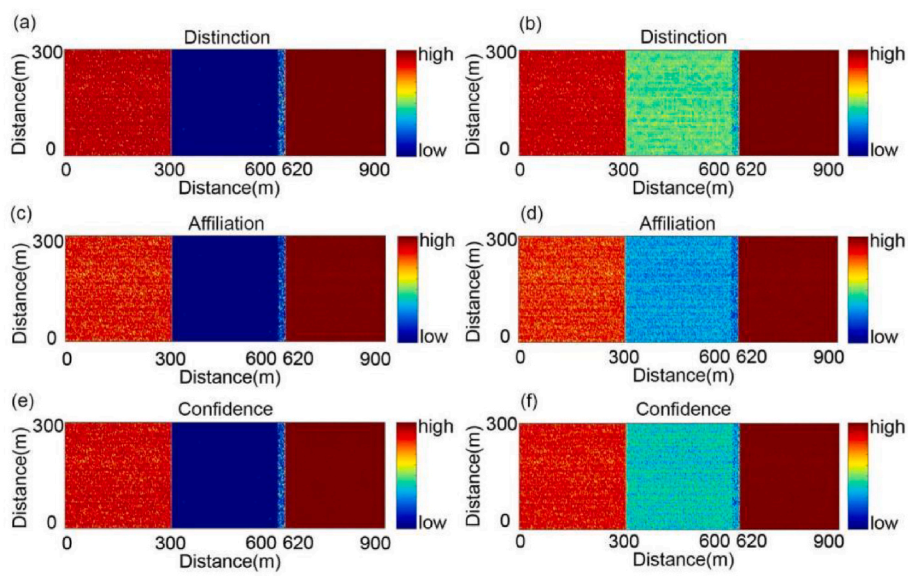

Fig. 4. For 2 dB synthetic prestack seismic data, (a), (c), and (e) show the Distinction, Affiliation, and Confidence corresponding to the facies maps obtained by the FCM method. (b), (d), and (f) correspond to the facies maps generated by FCM-CEC method.

$$\mathrm{P}(x_h = l | x_r = k) = \frac{1-\alpha}{K-1} \quad l, k \in \{1, 2, ..., K\} \text{ and } l \neq \mathrm{k} \tag{5}$$

Obviously, α represents the probability that x_h and x_r belong to the same cluster. Considering that there may be $K-1$ possibility when x_h and x_r do not belong to the same cluster, we can also calculate the probability that x_h and x_r belong to different clusters.

For the seismic signals of a pair of non-directly adjacent reflectors x_h and x_r, it is assumed that the Manhattan distance between them is n. We define $\mathrm{P_n}$ to represent the probability that x_h and x_r belong to the same cluster of seismic facies (similarly, the probability that a pair of reflectors with Manhattan distance $\mathrm{n}-1$ belong to the same cluster of seismic facies is $\mathrm{P_{n-1}}$). According to formulas (4) and (5), we can get the following recursive expression:

$$\mathrm{P_n} = \alpha \mathrm{P_{n-1}} + (K-1)\frac{1-\alpha}{K-1}\frac{(1-\mathrm{P_n})}{K-1} \tag{6}$$

Similarly, when $\mathrm{n} = 1$, then the two reflectors are adjacent reflectors, according to our definition and formula (4), we have:

$$\mathrm{P_1} = \alpha \tag{7}$$

Simultaneously deriving formulas (7) and (8), we can get:

$$\mathrm{P_n} = \left(\frac{K\alpha - 1}{K-1}\right)^{n-1}\left(\alpha - \frac{1}{K}\right) + \frac{1}{K} \tag{8}$$

Further, using the formula derived above, we can get the following equations:

$$\mathrm{P}(\mathrm{x_i} = \mathrm{k} | \mathrm{x_m} = \mathrm{k}, \mathrm{d} = \mathrm{n})\Big) = \left(\frac{K\alpha - 1}{K-1}\right)^{n-1}\left(\alpha - \frac{1}{K}\right) + \frac{1}{K} \quad \mathrm{k} \in \{1, 2, ..., K\} \tag{9}$$

$$P(x_i=l|x_m=k,d=n)=\frac{1-P(x_i=k|x_m=k,d=n)}{K-1}\quad l,k\in\{1,2,...,K\}\text{ and }l\neq k \tag{10}$$

Through formulas (9) and (10), we can obtain the correlation relationship between adjacent and non-adjacent reflection element seismic signals inferred from the perspective of probability. Among them, α is an important probability parameter we defined, which needs to be given. It directly characterizes the correlation of reflection elements in the first-order neighborhood, and its value affects our evaluation of the correlation of seismic signals of adjacent reflection elements. Therefore, a reasonable value of α is extremely important to us. In this paper, we use a more intuitive way to give the value of α:

$$\alpha=\frac{\sum_{i=1}^{N}\sum_{j\in \mathrm{Direct}\ (i)} I(x_i=x_j)}{\sum_{i=1}^{N}\sum_{j\in \mathrm{Direct}\ (i)} I(x_i=x_j)+\sum_{i=1}^{N}\sum_{j\in \mathrm{Direct}\ (i)} I(x_i\neq x_j)} \tag{11}$$

$$I(condition)=\begin{cases}1,\text{if } & condition=1\\0,\text{if } & condition=0\end{cases} \tag{12}$$

where $Direct(i)$ is one of the four reflection elements in the first-order neighborhood of reflection element x_i. Function $I(condition)$ is an indicator function, and its specific value is determined according to the actual situation.

Through formula (11), using the seismic data of the actual work area for estimation and calculation, the value of α is about 0.804. This indicates that the seismic signal features between adjacent reflectors in the formation have a positive mutual influence, that is, the same seismic facies has lateral continuity in the formation. So, in this paper, we set the value of the defined spatial information transfer factor α to be 0.8, and further apply it to our proposed FCM-CEC algorithm for seismic facies analysis.

In the FCM, the calculation of the probability of the membership u_{ik} of the sample to the cluster center is based on the feature relationship of all samples. The cluster relationship $P(x_i|x_m)$ between two reflectors we defined is based on the characteristic relationship of local reflector seismic signals. For two types of probability distributions $p(x)$ and $q(x)$, in information theory, cross-entropy is often used to measure the relationship between the two. The definition of cross-entropy is as follows:

$$H(p,q)=-\sum_{x\in X}p(x)\log(q(x)) \tag{13}$$

In recent years, cross-entropy as an objective function has been widely used in machine learning and deep learning to describe the gap between the predicted value of the model and the real value, and has achieved good results (Zhang et al., 2019). In this paper, we choose the cross entropy function as the distance measure between the two probability distributions of u_{ik} and $P(x_i|x_m)$. Thus, the objective function of the original FCM can be rewritten as:

$$J=\sum_{i=1}^{N}\sum_{k=1}^{K}u_{ik}^{q}\|x_i-v_k\|^2-\beta'\sum_{i=1}^{N}\sum_{k=1}^{K}u_{ik}{}^{q}\sum_{m\in N_i}\log\left(P(x_i|x_m)^q\right)=\sum_{i=1}^{N}\times\sum_{k=1}^{K}u_{ik}^{q}\|x_i-v_k\|^2-\beta\sum_{i=1}^{N}\sum_{k=1}^{K}u_{ik}{}^{q}\sum_{m\in N_i}\log(P(x_i|x_m)) \tag{14}$$

Here, $\beta=\beta' q$ is used as a weighting factor as a weight measure between feature consistency and stratigraphic lateral continuity for all samples in the clustering process. The minimal optimization of this objective function can be solved by using the Lagrange multiplier method. Among them, the two iterative update formulas of sample membership u_{ik} and cluster center v_k are as follows:

$$u_{ik}=\frac{\sum_{j=1}^{K}\left[\|x_i-v_j\|^2-\beta\sum_{m\in N(i)}\log(p_{mj})\right]^{\frac{1}{q-1}}}{\left[\|x_i-v_j\|^2-\beta\sum_{m\in N(i)}\log(p_{mk})\right]^{\frac{1}{q-1}}} \tag{15}$$

$$v_k=\frac{\sum_{i=1}^{N}(u_{ik})^q x_i}{\sum_{i=1}^{N}(u_{ik})^q} \tag{16}$$

Accordingly, the steps of the fuzzy c-means clustering algorithm with cross-entropy constraints we propose in this paper are shown in Algorithm 1.

Algorithm 1. Fuzzy c-means clustering with cross-entropy constraints (FCM-CEC)

Algorithm 1: Fuzzy c-means clustering with cross-entropy constraints (FCM-CEC)

Input: All samples x_i, number of clusters K, weighting index q, defined spatial information transfer factor α, window size N_i and optimization iteration stop threshold ε.

Output: Clustering result k_i for each sample.

Main program:

Step 1. Randomly initialize the cluster centers.

Step 2. Loop iteration until the termination condition is reached:

While max $|J_{new}-J_{old}|>\varepsilon$ **do:**

Update the membership matrix u_{ik} according to formula 15

Update the cluster center point v_k according to formula 16

Calculate the joint objective function value J

end

Step 3. When the iteration termination condition is reached to terminate the iteration, divide each sample xi into the category with the highest degree of membership.

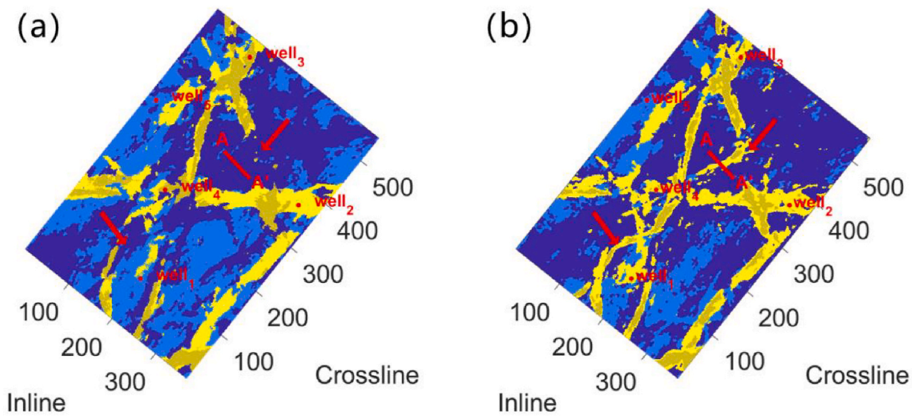

Fig. 5. Seismic facies maps of the original FCM(a) and FCM-CEC(b) applied to real data. The yellow and tan areas represent thin and thick sand bodies, respectively, while the light blue and dark blue areas represent the background. The red arrows indicate the areas interpreted as small river courses by the FCM-CEC method and as background by the FCM method.

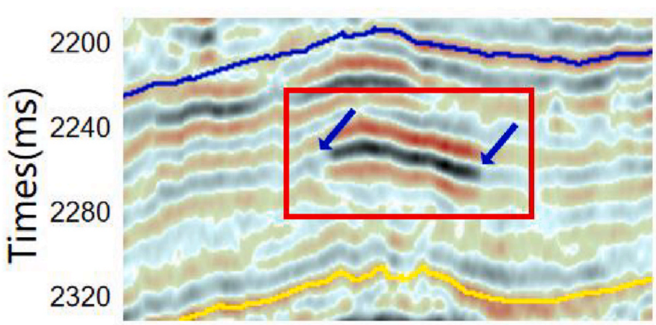

Fig. 6. The vertical seismic section along the line AA' in Fig. 5. "Bright spot" features along the target horizon can be observed in the red box. The presence of channels in this area is interpreted by experts, and the blue arrows indicate the edge of the channels.

3. Synthetic data examples

In order to facilitate the verification of the proposed method, we use synthetic seismic data for experimental verification. We design a layered stratigraphic model as shown in Fig. 2(a), which contains three layers of tectonic media, the first and third layers are mudstone structures, and the second layer is sand. Among them, the second layer contains three large seismic facies and a micro-fault. The geological model parameters of different tectonic media such as S-wave propagation velocity, P-wave propagation velocity, and medium density are shown in Fig. 2(b). In this paper, five different azimuths are selected, and the seismic reflection waveforms are inverted using the 35 Hz Ricker wavelet and the Aki-Richards approximation. The data sampling interval is 1 ms. Finally, we obtain synthetic pre-stack seismic data with 5 seismic traces per gather. We use a 50 ms window to capture the seismic profiles near the bottom of the second layer to analyze the seismic facies.

We add different Gaussian noise filtered in the seismic bandwidth (10–15 Hz 50–60 Hz) to the synthetic traces. The FCM and FCM-CEC algorithms are applied to the 6 dB, 4 dB, and 2 dB synthetic data, respectively. Fig. 3 shows the results of the two algorithms. By comparing (a), (c), and (e) in Fig. 3, we can see that when the noise increases, the recognition effect of the FCM algorithm decreases. For the same data set, the seismic facies maps generated by the FCM-CEC algorithm have enhanced the continuity inside the geological body, and the boundaries of the geological body are clearer. In the lower signal-to-noise ratio data (Fig. 3(e)), the FCM algorithm can no longer correctly identify the micro-fault in the formation, but the FCM-CEC algorithm has achieved a better result (Fig. 3(f)).

In order to quantitatively evaluate the clustering effect of the algorithm, this paper uses a confidence analysis proposed by Cai et al. (2019). Fig. 4 shows a visual comparison of Distinction, Affiliation, and Confidence for 2 dB data. It can be seen that, compared with the results of the FCM method, the FCM-CEC algorithm generally achieves higher Distinction, Affiliation, and Confidence. Tests on synthetic data demonstrate that our proposed method is more robust to noise.

4. Field data examples

The survey is in southwest China, with 551 survey lines, each of which has a total of 371 traces. The seismic data are 2 ms sampled, and the dominant frequency of the seismic data is 40Hz. We slice seismic data with a length of 40 ms along the target horizon. There are river channels along the target horizon, and the goal of the study is to determine the distribution and edges of the river channels. Similar to the synthetic data, we use the original FCM and FCM-CEC to analyze the structural slice, and the facies maps are shown in Fig. 5. In Fig. 5, the yellow and tan areas represent thin and thick sand bodies, respectively, while the light blue and dark blue areas represent the background. It can be seen that the yellow area outlines the boundaries of the river channel sand body, and there are thicker sand bodies (tan areas) in the center of the channels.

However, compared with the seismic facies map obtained by the FCM method (Fig. 5(a)), the seismic facies map obtained by the FCM-CEC method (Fig. 5(b)) has many more details of the channel edges, and reveals new small river courses. Line AA' (in Fig. 5) is selected in the study area, which crosses a channel identified only by the FCM-CEC method (interpreted as background in Fig. 5(a) and as channel in Fig. 5(b)). The vertical seismic section along the line AA' is shown in Fig. 6. "Bright spot" features can be observed in the seismic profile, indicating the presence and location of channel sand bodies. The blue arrows in Fig. 6 indicate the edges of the channel, according to the interpretation of experts. This means that the FCM-CEC method detects more channels, which can provide more information for the delineation of the lithologic body of interest. Moreover, there are five wells in our study area, which can provide lithology labels. Wells 1–4 encountered sand layers during the development stage, while Well 5 did not encounter sand bodies. Compared with Fig. 5(a), the FCM-CEC method (Fig. 5(b)) correctly predicts the lithology corresponding to Well 1, showing a higher coincidence rate with the wells.

Both the FCM and FCM-CEC methods are fuzzy clustering methods, that is, for each stratum reflection element, it will be assigned to the category with the highest degree of membership. Computing membership is an iterative process accompanied by updating of cluster centers (as shown in Algorithm 1). The FCM method will take into account the influence of all the data when updating the cluster center in each iteration, no matter how much the data is affected by the noise. However, the FCM-CEC method will take into account the constraints of the lateral continuity of the formation. Those data that are less affected by noise tend to have higher soft probability values in the early stages of algorithm iterations. They are more likely to be classified in the same category as adjacent reflectors and will play a more important role in the next iteration. On the other hand, the impact of data that is more affected by noise will be weakened with the iterative process. We believe that letting more reliable samples play a more important role in the clustering process is the reason why the FCM-CEC method can achieve better results.

5. Conclusions

The conventional seismic facies analysis methods are often purely data-driven approaches, ignoring the correlation between adjacent seismic gathers, making the seismic facies with poor lateral continuity. In this article, we propose the FCM-CEC method. A probabilistic model is developed to describe the correlation of adjacent formation reflectors. Then the lateral continuity of strata is added as priori information to the mode division of seismic reflection elements. Tests on synthetic data and real seismic data demonstrate the effectiveness of the proposed method. The seismic facies maps obtained by the FCM-CEC method have better consistency within the geological body and less uncertainty on the boundary. Moreover, the proposed method can obtain more information about the lithologic body of interest.

Declaration of competing interest

The authors declare that they have no known competing financial interests or personal relationships that could have appeared to influence the work reported in this paper.

References

Alsadi, H.N., 2016. Seismic Hydrocarbon Exploration: 2D and 3D Techniques[M]. Springer.
Cai, H., Wu, Q., Ren, H., et al., 2019. Pre-stack texture based semi-supervised seismic facies analysis using global optimization[J]. J. Seismic Explor. 28, 513–532.
Gao, Y., Zhao, P., Li, G., et al., 2021. Seismic noise attenuation by signal reconstruction: an unsupervised machine learning approach[J]. Geophys. Prospect. 69 (5), 984–1002.
Li, J., Wu, X., Ye, Y., et al., 2022. Unsupervised contrastive learning for seismic facies characterization[J]. Geophysics 88 (1), WA81–WA89.
Liu, S., Jin, S., Chen, Q., 2022. Three-dimensional gravity inversion based on optimization processing from edge detection[J]. Geodesy and Geodynamics.
Mirzakhanian, M., Hashemi, H., 2022. Semi-supervised fuzzy clustering for facies analysis using EEI seismic attributes[J]. Geophysics 87 (4), 1–43, 2022, 13(5): 503-524.
Mousavi, S.M., Zhu, W., Ellsworth, W., et al., 2019. Unsupervised clustering of seismic signals using deep convolutional autoencoders[J]. Geosci. Rem. Sens. Lett. IEEE 16 (11), 1693–1697.
Qian, F., Yin, M., Liu, X.Y., et al., 2018. Unsupervised seismic facies analysis via deep convolutional autoencoders[J]. Geophysics 83 (3), A39–A43.
Su-Mei, H., Zhao-Hui, S., Meng-Ke, Z., et al., 2022. Incremental semi-supervised learning for intelligent seismic facies identification[J]. Appl. Geophys. 19 (1), 41–52.
Xu, G., Haq, B.U., 2022. Seismic facies analysis: past, present and future[J]. Earth Sci. Rev. 224, 103876.
Zhang, K., Wang, X., Guo, Y., et al., 2019. Competing ratio loss for multi-class image classification[C]. 2019 IEEE Visual Communications and Image Processing (VCIP) 1–4. IEEE.